



## MODIFIED BRIDGELESS CONVERTER FED EV BATTERY CHARGER WITH IMPROVED POWER FACTOR

<sup>1</sup>Bugga Shailaja, :M.Tech(PEED), Mahatma Gandhi institute of technology, Gandipet, Hyderabad, Telangana 500075, [bshailaja\\_pgeee215402@mgit.ac.in](mailto:bshailaja_pgeee215402@mgit.ac.in)

<sup>2</sup>Mrs.N.Madhuri(Mtech) Assistant professor, Electrical and electronics engineering (Power electronics), Mahatma Gandhi institute of technology, kokapet(Village), Gandipet (Mandal), Hyderabad, 500075, Telangana, [nmadhuri\\_eee@mgit.ac.in](mailto:nmadhuri_eee@mgit.ac.in)

### Abstract

Electric vehicles (EVs) rely on rechargeable batteries to generate the required traction force. Typically, these batteries are recharged using an AC–DC converter referred to as an EV charger. The standard architecture of an EV battery charger consists of a boost converter at the front-end and an isolated converter in the subsequent stage. The utilization of a full-wave Diode Bridge at the charger's input introduces a significant amount of harmonic distortion (55.3%) in the input current during the battery charging process, leading to a poor source power factor. Furthermore, the non-sinusoidal shape of the input current results in an increased displacement between the source voltage and current. Consequently, this reduces system losses and enhances efficiency by minimizing conduction loss without a diode bridge at the charger's input. The adoption of the bridgeless technique enables current conduction through fewer semiconductor components, thereby reducing losses and improving the overall efficiency of the charger. To achieve this, a charger based on a modified bridgeless Landsman power factor correction converter, preceded by a flyback converter, will be designed and simulated using MATLAB/Simulink.

**Keywords:** EV Battery Charger Power Factor Improvement Electric Vehicles (EVs) Rechargeable Batteries AC–DC Converter Boost Converter Isolated Converter Diode Bridge Harmonic Distortion

### Introduction

Given the stringent oversight on emissions, fuel conservation, global warming, and limited energy resources, the role of electric mobility is crucial in advancing sustainable and efficient alternatives in the transportation sector. To address this, a survey has been conducted, examining the current scenario and future technologies for electric vehicle (EV) propulsion. Electric mobility offers several advantages over traditional petrol- and diesel-powered vehicles. However, comprehensive attention from researchers is necessary to fully integrate transportation electrification. Effective control strategies must be devised to seamlessly integrate electric mobility with the existing distribution system. Some of these strategies are linked to power quality issues addressed by EV chargers involved in the battery charging process. Rechargeable batteries power EVs to provide the necessary traction force, with typical recharging involving an AC–DC converter known as an EV charger. However, interleaving the

PFC converter comes at the cost of high current stress on switches. The full-bridge topology is prominent for PFC-based EV chargers due to high power density and efficiency, but the control complexity arises from the arrangement of four switches. An LLC (Inductor–Inductor–Capacitor) resonant converter offers an attractive solution with high efficiency, low Electromagnetic Interference (EMI) noise, and highpower density across a wide input range. However, the design and analysis complexity of the LLC converter has led to its substitution by unidirectional or bidirectional AC-DC converters in integrated on-board or off-board configurations. Highlighting AC-DC conversion as a distinctive feature of EV battery chargers, many Diode Bridge Rectifier (DBR)-fed unidirectional isolated single-stage or two-stage converters without isolation have been identified. In this context, Figure 1(a) illustrates the configuration of a classic single-phase DBR-fed unidirectional E-rickshaw battery charger, with the corresponding specifications of the observed E-rickshaw provided in Table I. However, the performance of the conventional charger does not align with the prescribed power quality (PQ) standard IEC 61000-3-2, as depicted in Figure 1(b). The presence of a full-wave diode bridge at the charger's input generates a substantial amount of harmonic distortion (55.3%) in the input current during the battery charging process, leading to a poor source power factor. Additionally, the non-sinusoidal shape of the input current increases the displacement between source voltage and current. Therefore, an efficient Power Factor Correction (PFC) technique is required at the front-end of the conventional DBR-fed charger to eliminate the adverse effects of the input DBR.

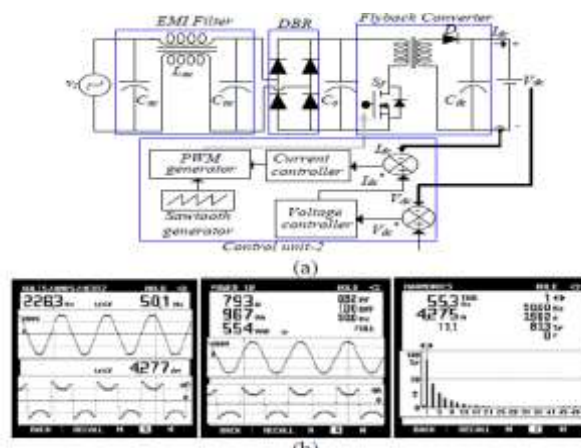


Figure. 1 Conventional E-Rickshaw Battery Charger: (a) Configuration (b) Measured input current, input power and THD in input current

Parameter	specification
Speed	0-25 Kmh in Power Mode
Range	120 Km/Charge
Battery Type	12V/100 Ah (4 Battery)
Motor Type	48V.850 W-1000W BLDC Motor
Brakes	Drum Type (Front & Rear)
Front Wheel	12"



Rear Wheel	14”
Charger	48V DC.10 Amp. (220V AC)
Charging Time	5-8 Hours
Loading Capacity	Up to 4-5 Passengers

Table 1. Specification of E-Rickshaw under consideration

## Literature Review

Wencong Su & Habiballah Eichi et al [1]: The development of a robust charging infrastructure is a crucial element essential for accommodating and supporting the successful deployment of Electric Vehicles (EVs). According to a recent report from the Massachusetts Institute of Technology (MIT), establishing a nationwide EV infrastructure appears to pose a greater challenge than producing affordable batteries to power these vehicles.

Ching Chuen Chan et al [2]: Conventional Internal Combustion Engine (ICE) vehicles have been in existence for over a century. With the global population increasing, the demand for personal transportation vehicles has dramatically risen in the past decade. This upward trend is expected to intensify as developing countries like China, India, and Mexico catch up. The demand for oil has also seen a significant increase.

The escalating use of personal vehicles brings forth the issue of emissions and contributes to the greenhouse effect, commonly known as global warming. The energy crisis has led to increased tensions in certain parts of the world. Government agencies and organizations have responded by implementing more stringent standards for fuel consumption and emissions. Despite advancements in Internal Combustion Engine (ICE) technology over the past century, further improvements, particularly in fuel economy and emission reduction, will depend on alternative evolutionary approaches.

Clement-Nyns et al. [3] assessed the impact of Plug-in Hybrid Electric Vehicles (PHEVs) on a residential distribution grid. Su et al. [4] examined the effects of integrating Plug-in Hybrid Electric Vehicles (PHEVs) and Plug-in Electric Vehicles (PEVs) into power grids, considering various charging scenarios. Roe et al. [5] conducted an investigation into how Plug-in Hybrid Electric Vehicles (PHEVs) could impact the electric power system, with a specific focus on power system infrastructure.

Dyke et al. [6] established a set of well-defined Electric Vehicle (EV) loads, which they subsequently used to analyze electrical energy usage and storage in the context of increasingly electrified road transportation.

## Methodology

### 3. CONVERTERS

#### 3.1 BUCK CONVERTER

A buck converter is a DC-to-DC step-down converter, resembling the design of a boost converter. Similar to the boost converter, it operates as a switched-mode power supply utilizing

two switches (a transistor and a diode), along with an inductor and a capacitor. While a voltage divider circuit is a simple means of reducing DC voltage, it is inefficient and lacks voltage regulation, leading to energy wastage [7]. In contrast, buck converters are highly efficient, with integrated circuits achieving up to 95% efficiency. They are also self-regulating, making them ideal for tasks such as converting the typical 12–24 V battery voltage in a laptop to the lower voltage required by the processor [8].

Theory of operation

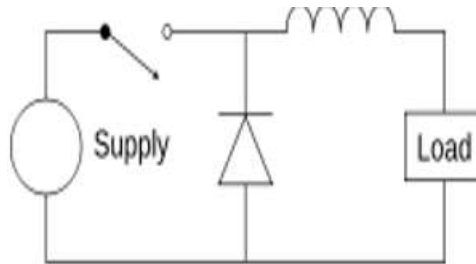


Figure 2 Buck converter circuit diagram

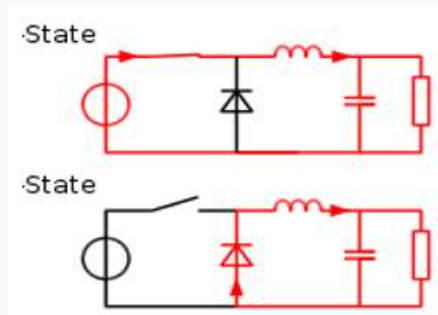


Figure 3 The two circuit configurations of a buck converter: On-state, when the switch is closed, and Off-state, when the switch is open

### 3.1.1 CONTINUOUS MODE

In continuous mode, a buck converter ensures that the current through the inductor ( $I_L$ ) never reaches zero during the commutation cycle [9]. The operating principle is illustrated by the chronogram.

The energy stored in inductor  $L$  is

$$E = \frac{1}{2} L \times I_L^2$$

The rate of change of  $I_L$  can be calculated from

$$V_L = L \frac{dI_L}{dt}$$

The increase in current during the On-state is given by:

$$\Delta I_{L_{on}} = \int_0^{t_{on}} \frac{V_L}{L} dt = \frac{(V_i - V_0)}{L} t_{on}$$

The decrease in current during the Off-state is given by:

$$\Delta I_{L_{off}} = \int_0^{t_{off}} \frac{V_L}{L} dt = -\frac{V_0}{L} t_{off}$$

So, we can write the equation as,

$$\frac{(V_i - V_0)}{L} t_{on} = \frac{V_0}{L} t_{off} = 0$$

### 3.1.2 DISCONTINUOUS MODE

Sometimes, the load's energy requirement is sufficiently low to be transferred within a duration shorter than the entire commutation period. In such instances, the inductor's current drops to zero during a portion of the period [10]. The only variation in the previously explained principle is that the inductor is fully discharged by the end of the commutation cycle. This, however, influences the earlier equations to some extent.

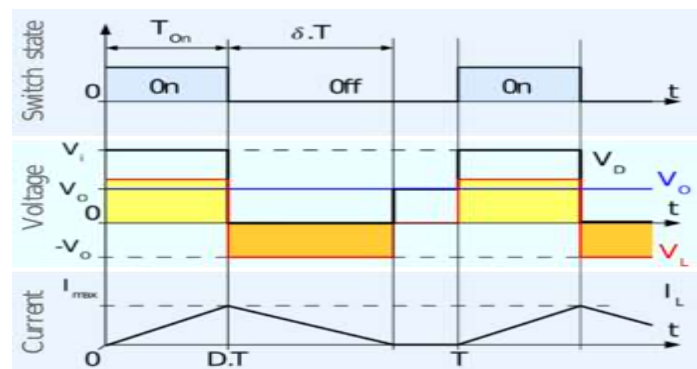


Figure 4 Time-dependent voltage & current evolution in a perfect discontinuous mode buck converter.

The Buck-Boost converter is an efficient and versatile power electronics solution that can step up or down voltage levels within a single topology. Its flexibility with variable input and output voltages makes it ideal for diverse applications like battery-powered devices, renewable energy systems, and LED drivers [11]. The Buck converter, a fundamental and widely-used topology, excels in voltage step-down applications due to its simplicity, high efficiency, and fast transient response. This makes it a popular choice in devices like DC-DC converters, voltage regulators, and power supplies [12]. Meanwhile, the Flyback converter is a cost-effective solution for isolated power supply needs. Its inherent capability for galvanic isolation suits applications with safety and voltage isolation requirements, such as power adapters, battery chargers, and LED drivers [13].

## 4 Modified Bridgeless Landsman Converter

### 4.1 PRINCIPLE OF OPERATION OF MODIFIED BL CONVERTER FED CHAREGR



The proposed modified Landsman converter fed battery charger comprises two stages: a modified BL converter for enhanced input wave-shaping and an isolated converter for EV battery charging under constant current (CC) constant voltage (CV) conditions [14]. The converter's operation is selected in DCM or CCM mode based on the application's requirement for low cost or low device stress, respectively. Considering the current emphasis on cost in battery chargers, a DCM mode is adopted [15]. Additionally, the flyback converter operates in the discontinuous region of the switching cycle, reducing the number of sensors in the circuit for battery control and minimizing size issues.

### A. Proposed Scheme:

Introduces a BL converter fed EV battery charger with regulated DC link voltage at an intermediate stage. The charger's input side is powered by a single-phase AC source. Two Landsman converters eliminate the input DBR, operating in parallel during the positive and negative half lines, respectively [16]. This reduces conduction losses by half as fewer components conduct in one switching cycle. To enhance performance-based switching, two synchronized converters switch at 20 kHz. The currents in output inductors ( $L_{op}$  and  $L_{on}$ ) are designed to become discontinuous over one switching cycle during positive and negative half-line operations [17]. This achieves control simplicity with a single sensor used to sense the intermediate output voltage.

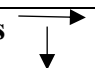
<b>Configuration</b>	<b>Conventional Charger (No PFC)</b>	<b>Conventional Charger (DBR +PFC)</b>	<b>Proposed BL Converter Fed Charger</b>
<b>Attributes</b> 			
Number of components	less	more	Increased
Control (with PFC)	-	Voltage Follower	Voltage Follower
Control (Battery)	Complex	Simple (dual PI)	Simple (dual PI)
Sensor (with PFC)	-	1 for output voltage	1 for output voltage
Losses (with DBR & PFC)	-	6.5% of total power	5.88% of total power
PFC	-	yes	yes
Power density	-	0.472 kW/kg	0.369kW/kg
PFC converter cost	-	43.11 \$	74.12\$
PFC sensors & DSP Cost	-	130.4\$	130.4\$
Mass	1.3 kg	1.8kg	2.3kg
Volume	1.21	1.51	2.11



TABLE II: Benchmarking the suggested bridge-less converter-fed EV charger against the traditional charger in terms of performance

**B. Function of the Proportional Term**

Similar to the P-Only controller, the proportional term of the PI controller,  $K_c \cdot e(t)$ , adjusts CO bias by adding or subtracting based on the current controller error,  $e(t)$ , at each time  $t$ . The adjustment is immediate and proportionate to the growth or reduction of  $e(t)$ . The past history and current trajectory of the controller error do not impact the computation of the proportional term [18]. The accompanying plot (click for a larger view) demonstrates this concept in a set-point response, displaying the error used in the proportional calculation.

- At time  $t = 25$  min,  $e(25) = 60 - 56 = 4$
- At time  $t = 40$  min,  $e(40) = 60 - 62 = -2$

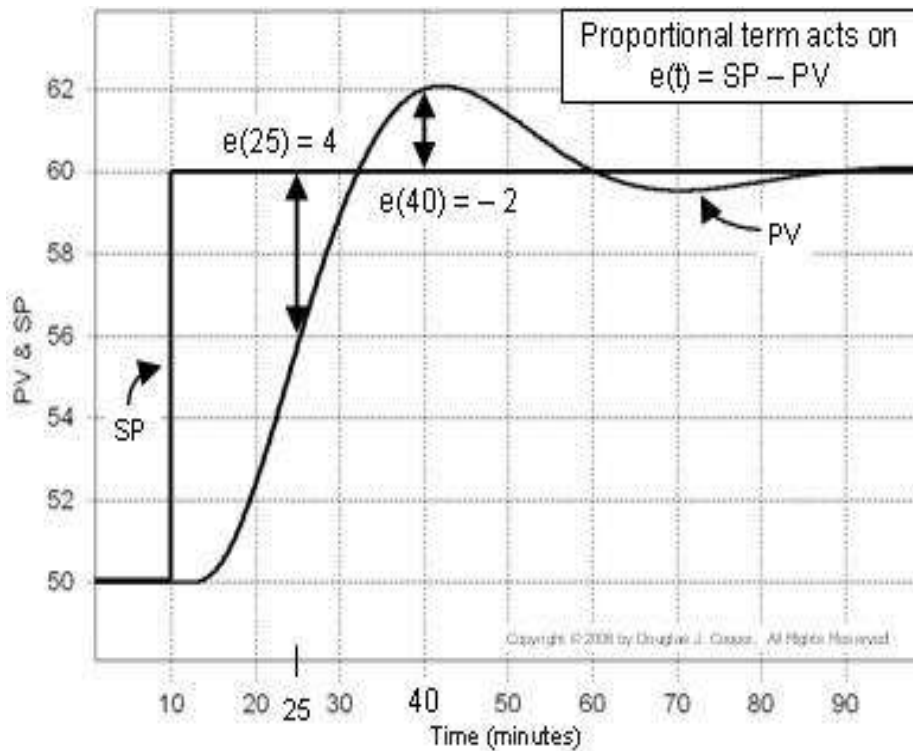


Figure 5. model accuracy comparison

**C. Function of the Integral Term**

While the proportional term assesses the current size of  $e(t)$  at the controller calculation time, the integral term considers the error's history—how long and how far the measured process variable has deviated from the set point over time. Integration involves continuous summation, accumulating the complete history of controller errors from the controller's initiation in automatic mode. The controller error is represented as  $e(t) = SP - PV$ . In the accompanying

plot (click for a larger view), the integral sum of error is computed as the shaded areas between the set point (SP) and process variable (PV) traces.

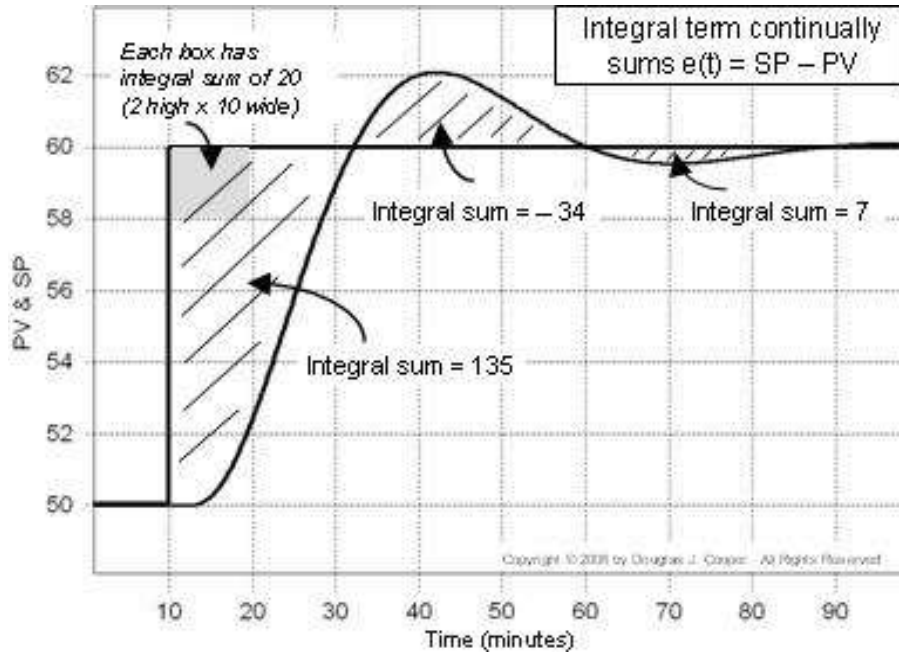


Figure 6. model measures estimation

A bridgeless converter is a power electronics circuit that eliminates the conventional diode bridge rectifier in power supply setups. Traditionally, diode bridges rectify AC to DC, but the bridgeless converter aims to minimize conduction losses associated with diode bridges, enhancing overall power conversion efficiency. In the standard diode bridge rectifier, voltage drops across diodes cause power losses. Bridgeless converters utilize alternative configurations, incorporating switches and control techniques to achieve rectification without diode bridges. This leads to reduced conduction losses and potentially improved power factor.

#### D. PI CONTROLLER

Figure 7 displays the PI speed controller's overall block diagram.

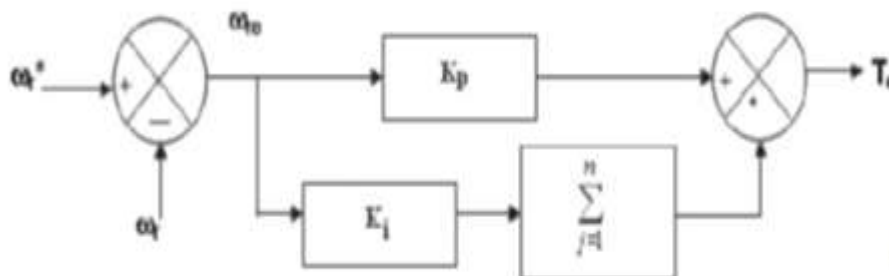


Figure 7. Block Diagram of PI Speed Controller

**Components and Interactions:**





**AC Power Input:** Represents the system's input from the AC power grid. **Bridgeless Landsman Converter:** An enhanced Landsman converter designed for efficient rectification. Incorporates power switches, diodes, and relevant control circuitry.

**Control System:** Implements a control algorithm for precise converter regulation. Control signals adjust switching frequency and duty cycle for optimal performance. Includes a Power Factor Correction (PFC) algorithm for enhanced power factor.

**EV Battery Model:** Simulates the electric vehicle battery, capturing voltage, current, and internal resistance characteristics. May include State of Charge (SOC) estimation for realistic behaviour.

**Feedback Loop:** Connects converter output and actual battery state to enable closed-loop control.

**Power Factor Measurement Block:** Monitors current and voltage to calculate the power factor. Provides continuous feedback to enhance system efficiency.

**Operation: Initialization:** Simulation begins with setup of initial conditions and models. AC

**Power Conversion:** The modified bridgeless Landsman converter rectifies AC power for EV battery charging.

**Control System Operation:** Parameters are adjusted based on feedback from the battery and power factor measurement block.

**Battery Charging:** Regulated output from the converter charges the EV battery.

**Power Factor Improvement:** Continuous optimization by the power factor correction algorithm enhances overall system power factor.

**Simulation Analysis:** Simulink records and analyzes performance indicators, including input/output waveforms, battery charging characteristics, and power factor improvements.

### **Result:**

The MATLAB/Simulink simulation for the modified bridgeless Landsman converter-fed EV battery charger illustrates the effectiveness of proposed modifications in achieving efficient, high-power-factor charging for electric vehicles. Simulation results offer insights into system dynamics, showcasing the impact of modifications on charging performance and power quality.

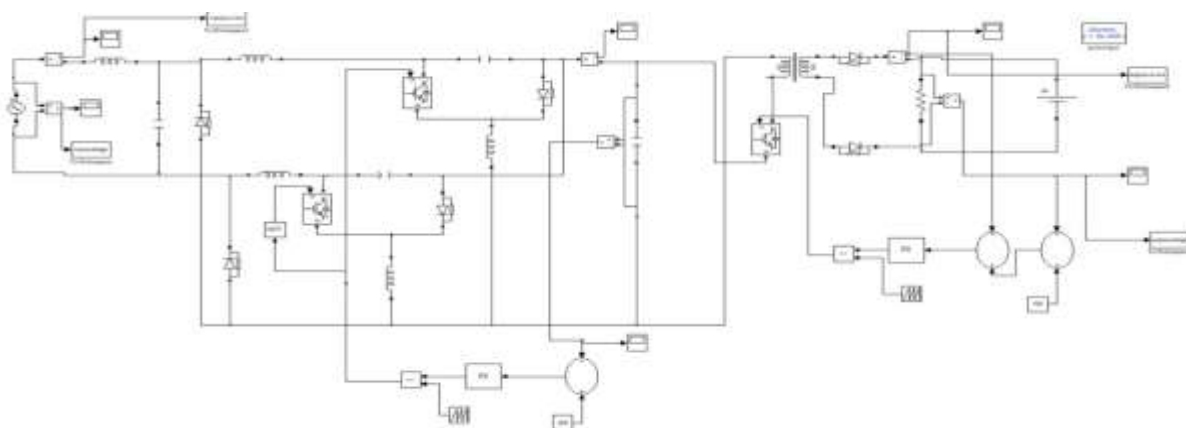


Figure 8 shows a simulation schematic for an enhanced power factor EV battery charger fed by a modified bridgeless converter.

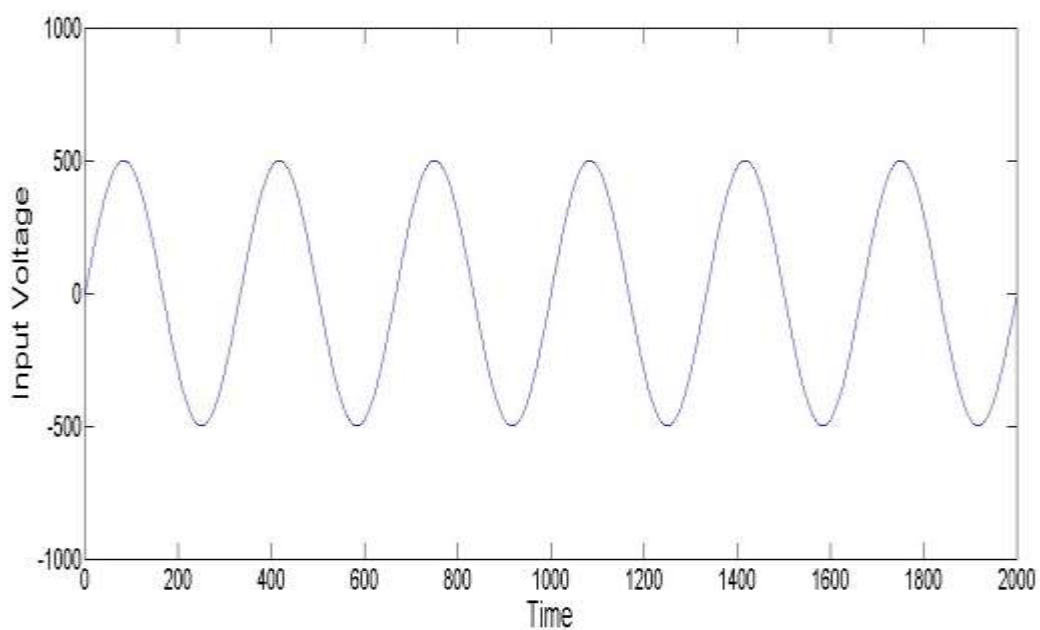


Figure 9 Input voltage wave forms

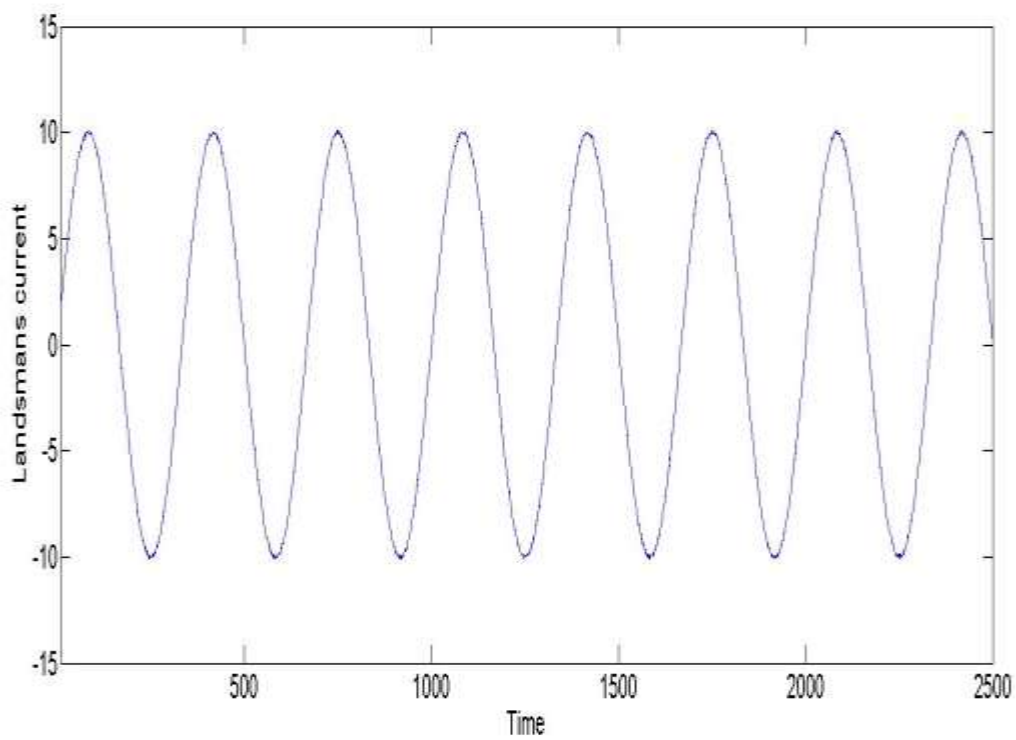


Figure 10 Input current wave form

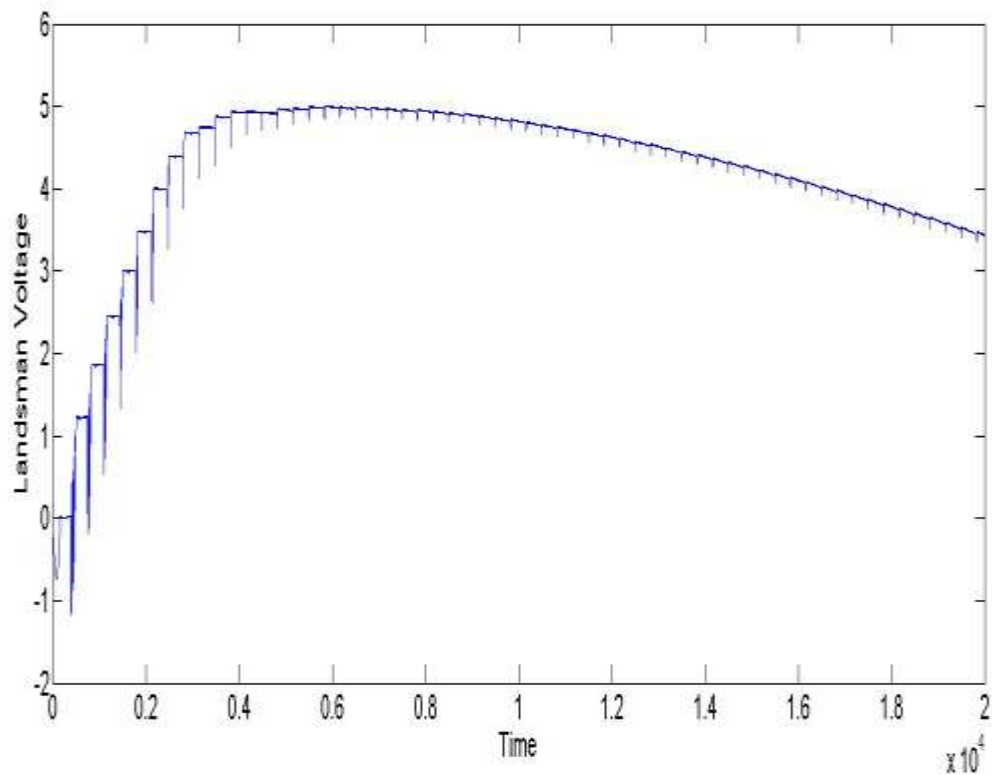


Figure 11 Landsman voltage

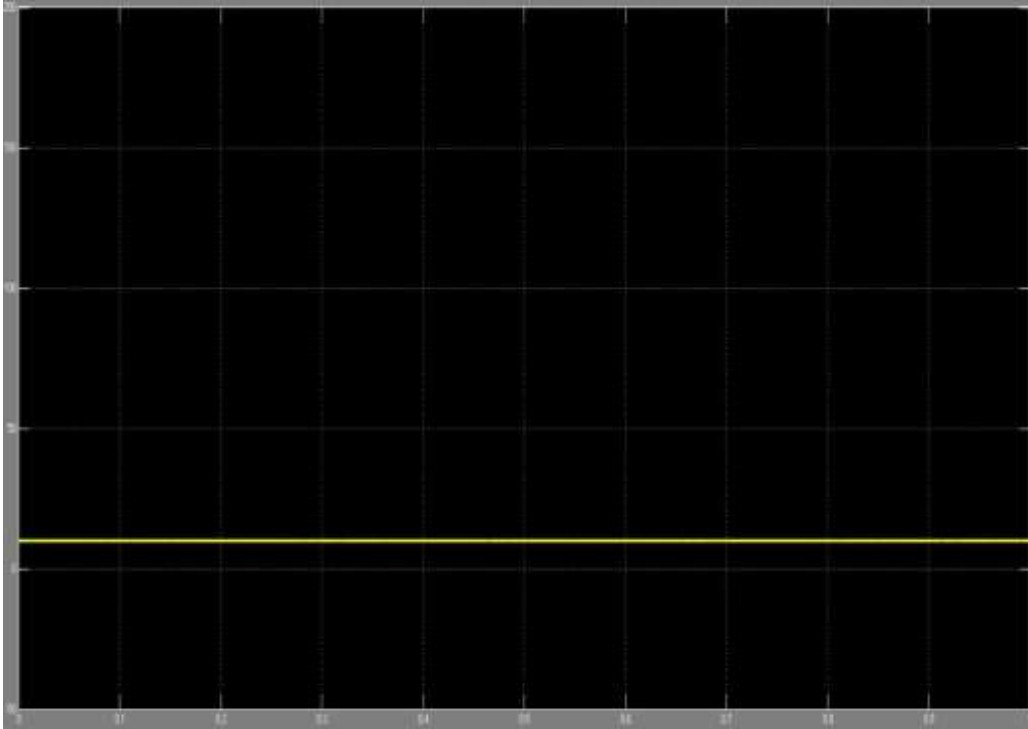


Figure 12 Output current fly back converter

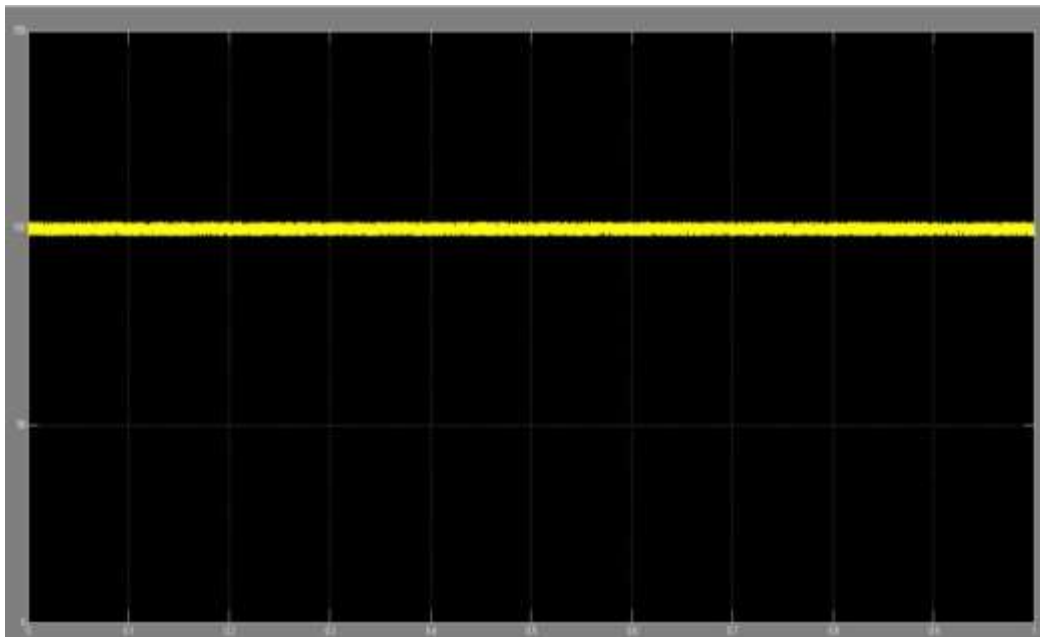


Figure 13 Output voltage fly back converter

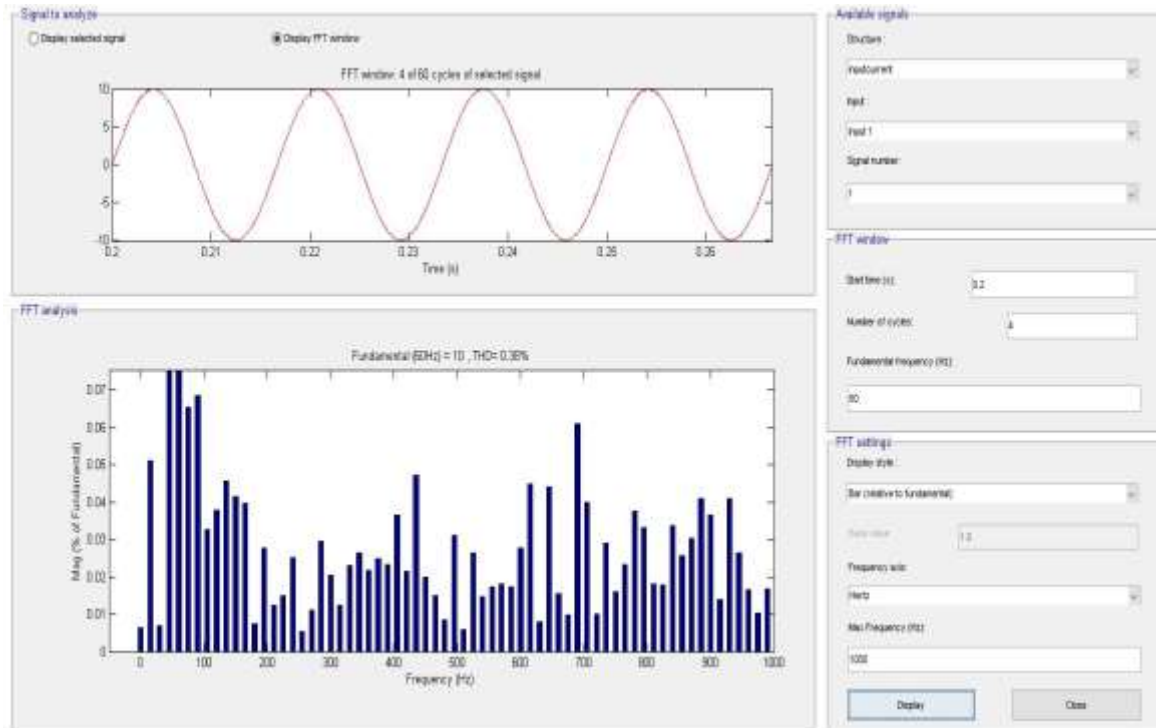


Figure 14 THD of Modified bridgeless converter fed EV battery charger with improved power factor

## CONCLUSION

This study proposes, analyses, and validates an enhanced EV charger featuring a modified BL Landsman converter followed by a flyback converter, providing inherent Power Factor Correction for EV battery charging. The designed and controlled EV charger in Discontinuous Conduction Mode (DCM) offers the advantage of fewer output sensors. The proposed BL converter reduces input and output current ripples. Experimental results from a prototype verify the charger's operation under steady state and sudden input voltage fluctuations. Hardware validation indicates satisfactory performance, ensuring improved power quality for EV battery charging. Furthermore, the proposed charger achieves a low input current Total Harmonic Distortion (THD) of 4.3%, meeting IEC 61000-3-2 standards for power quality. Thus, the BL converter-fed charger presents a cost-effective, reliable alternative to replace conventional, inefficient EV battery chargers.

## REFERENCES

- [1] WencongSu, HabiballahEichi, Wenten Zeng and Mo-Yuen Chow, "A survey on the electrification of transportation in a smart grid environment," IEEE Transactions Industrial Informatics, vol. 8, no. 1, pp. 1-10, Feb. 2012.



- [2] Ching Chuen Chan, "The state of the art of electric, hybrid, and fuel cell vehicles," *Proc. IEEE*, vol. 95, no. 4, pp. 704–718, Apr. 2007.
- [3] Kaushik Rajashekara, "Present status and future trends in electric vehicle propulsion technologies," *IEEE J. Emerg. Sel. Topics Power Electronics.*, vol. 1, no. 1, pp. 3–10, Mar. 2013.
- [4] Juan C. Gomez and Medhat M. Morcos, "Impact of EV battery chargers on the power quality of distribution systems," *IEEE Transactions Power Del.*, vol. 18, no. 3, pp. 975–981, Jul. 2003.
- [5] Luca Solero, "Nonconventional on-board charger for electric vehicle propulsion batteries," *IEEE Transactions Vehicular Technology*, vol. 50, no. 1, pp. 144-149, Jan 2001.
- [6] Devendra Patel and Vivek Agarwal, "Compact onboard single phase EV battery charger with novel low-frequency ripple compensator and optimum filter design," *IEEE Transactions Vehicular Technology*, vol. 65, no. 4, pp. 1948-1956, April 2016.
- [7] Hye-Jin Kim, Gab-SuSeo, Bo-Hyung Cho, and Hangseok Choi, "A simple average current control with on-time doubler for multiphase CCM PFC converter," *IEEE Trans. Power Electron.*, vol. 30, no. 3, pp. 1683–1693, Mar. 2015.
- [8] Adria Marcos-Pastor, Enric Vidal-Idiarte, Angel Cid-Pastor and L. Martinez-Salamero, "Interleaved digital power factor correction based on the sliding-mode approach," *IEEE Transactions Power Electronics*, vol. 31, no. 6, pp. 4641-4653, June 2016.
- [9] MuntasirAlam, Wilson Eberle, Deepak S. Gautam and Chris Botting, "A soft-switching bridgeless AC–DC power factor correction converter," *IEEE Transactions Power Electronics*, vol. 32, no. 10, pp. 7716-7726, Oct. 2017.
- [10] Siddharth Kulasekaran and Raja Ayyanar, "A 500-kHz, 3.3-kW power factor correction circuit with low-loss auxiliary ZVT circuit," *IEEE Transactions Power Electronics*, vol. 33, no. 6, pp. 4783-4795, June 2018.
- [11] Jae-Hyun Kim, Chong-Eun Kim, Jae-Kuk Kim, Jae-Bum Lee, and Gun-Woo Moon, "Analysis on load-adaptive phase-shift control for high efficiency full-bridge LLC resonant converter under light load conditions," *IEEE Trans. Power Electron.*, vol. 31, no. 7, pp. 4942–4955, Jul. 2016.
- [12] Chuan Shi, Haoyu Wang, Serkan Dusmez and Alireza Khaligh, "A SiC-based high-efficiency isolated onboard PEV charger with ultrawide DC-link voltage range," *IEEE Transactions Industry Applications*, vol. 53, no. 1, pp. 501-511, Jan.-Feb. 2017.
- [13] Junjun Deng, Siqi Li, Sideng Hu, Chunting C. Mi and Ruiqing Ma, "Design methodology of LLC resonant converters for electric vehicle battery chargers," *IEEE Transactions Vehicular Technology*, vol. 63, no. 4, pp. 1581-1592, May 2014.
- [14] Chuan Shi, Yichao Tang and Alireza Khaligh, "A single-phase integrated onboard battery charger using propulsion system for plug-in electric vehicles," *IEEE Transactions Vehicular Technology*, vol. 66, no. 12, pp. 10899-10910, Dec. 2017.
- [15] Bhim Singh, Sanjeev Singh, Ambarish Chandra and Kamal AlHaddad, "Comprehensive study of single-phase AC-DC power factor corrected converters with





high-frequency isolation,” IEEE Transactions Industrial Informatics, vol. 7, no. 4, pp. 540-556, Nov. 2011.

- [16] Limits for Harmonics Current Emissions (Equipment current  $\leq 16A$  per Phase), International standards IEC 61000-3-2, 2000.